Title

Long-term aging and degradation of microplastic particles: Comparing in situ oceanic and experimental weathering patterns

Journal

Marine Pollution Bulletin, 110(1)

ISSN

0025-326X

Authors

Brandon, Jennifer
Goldstein, Miriam
Ohman, Mark D

Publication Date

2016-09-01

DOI

10.1016/j.marpolbul.2016.06.048

Peer reviewed

Marine Pollution Bulletin xxx (2016) xxx-xxx

Contents lists available at ScienceDirect

Marine Pollution Bulletin

journal homepage: www.elsevier.com

Long-term aging and degradation of microplastic particles: Comparing in situ oceanic and experimental weathering patterns

Jennifer Brandon,* Miriam Goldstein, Mark D. Ohman

Scripps Institution of Oceanography, University of California San Diego, La Jolla, CA 92093, USA

ARTICLE INFO

Article history:
Received 28 June 2015
Received in revised form 2 June 2016
Accepted 12 June 2016
Available online xxx

Keywords:
FTIR
Polyethylene (PE)
Polypropylene (PP)
North Pacific Subtropical Gyre
Weathering
Oceanic microplastic

ABSTRACT

Polypropylene, low-density polyethylene, and high-density polyethylene pre-production plastic pellets were weathered for three years in three experimental treatments: dry/sunlight, seawater/sunlight, and seawater/darkness. Changes in chemical bond structures (hydroxyl, carbonyl groups and carbon-oxygen) with weathering were measured via Fourier Transform Infrared (FTIR) spectroscopy. These indices from experimentally weathered particles were compared to microplastic particles collected from oceanic surface waters in the California Current, the North Pacific Subtropical Gyre, and the transition region between the two, in order to estimate the exposure time of the oceanic plastics. Although chemical bonds exhibited some nonlinear changes with environmental exposure, they can potentially approximate the weathering time of some plastics, especially high-density polyethylene. The majority of the North Pacific Subtropical Gyre polyethylene particles we measured have inferred exposure times > 18 months, with some > 30 months. Inferred particle weathering times are consistent with ocean circulation models suggesting a long residence time in the open ocean.

1. Introduction

Plastics in the ocean, particularly in the North Pacific Subtropical Gyre, have been of concern for decades (Carpenter and Smith, 1972; Wong et al., 1974). Recent studies estimate that there may be approximately five trillion pieces of plastic in the global ocean, with an estimated 4.8 to 12.7 million metric tons entering the ocean annually (Eriksen et al., 2014; Jambeck et al., 2015). Eriksen et al. (2014), along with others (Hidalgo-Ruz et al., 2012; Goldstein et al., 2013), state that the vast numerical majority of plastics in the ocean are microplastic, or particles < 5 mm in diameter. However, there is currently no method that estimates how long a given microplastic particle has been in the ocean. The small size of fragmented, weathered particles also makes it impossible to trace these particles to their source (Jambeck et al., 2015). Knowing how long a particle has been in the ocean is critical for calculating the residence time of particles in different regions of the ocean, testing the accuracy of models, and assessing the efficacy of marine debris mitigation policy.

The small fragments of microplastic created by weathering are detrimental to ocean ecosystems for multiple reasons. Studies have shown gooseneck barnacles (Goldstein and Goodwin, 2013), mesopelagic fishes (Davison and Asch, 2011), Norway lobsters (Murray and Cowie, 2011), and other small animals can consume microplastics *in situ*, and other invertebrates have been shown to eat them in lab settings (Murray and Cowie, 2011; Cole et al., 2013; Wright et al., 2013). Synthetic microfibers and microplastics are small enough to physically accumulate and to translocate from an organism's gut into its circulatory system (Browne et al., 2008). Some plastics contain harmful chemical additives (e.g. PCBs – polychlorinated biphenyls) that can bioaccumulate in marine organisms, leading to liver toxicity and other deleterious physiological effects (Rochman et al., 2013). Since plastics' hydrophobicity causes them to sorb marine and atmospheric persistent organic pollutants, there is also concern for bioaccumulation of these pollutants from plastic ingestion (Ogata et al., 2009).

Microplastics are currently impossible to remove *en masse* from the open ocean due to their small size, chemical inertness, similar dimension and distribution as plankton and fish eggs, and their distribution over the vast extent of the oceanic gyres. Thus, it is essential to understand processes that lead to the accumulation and degradation of plastic particles, as well as to develop strategies to limit inputs into the ocean (Jambeck et al., 2015).

Although many studies have examined aging of polyethylene and polypropylene (Stark and Matuana, 2004; La Mantia and Morreale, 2008), almost all have been conducted in accelerated weathering devices that use much higher temperatures than natural weathering (Stark and Matuana, 2004). Elevated temperatures can lead to different chemical reactions than those that occur naturally (Lacoste and Carlsson, 1992; Tidjani, 2000).

There have been some studies of the natural weathering of plastics: Andrady et al. (1993) examined natural weathering of LDPE, and Rajakumar et al. (2009) examined natural weathering of PP; both experiments tested sheets of plastic film in ambient air and rain. Andrady (1990) compared the weathering of LDPE films in ambient air and ambient seawater. Pegram and Andrady (1989) tested LDPE film, PP strapping tape, latex balloons and trawl netting in both ambient air and seawater. Though these studies are very useful, the numerical majority of marine debris is not intact films or objects but rather

* Corresponding author.
Email address: jabrandon@ucsd.edu (J. Brandon)

http://dx.doi.org/10.1016/j.marpolbul.2016.06.048
0025-326/

microplastic particles (Goldstein et al., 2013). Also, most previous studies extend for a maximum of three months, with some for only a few weeks (Lacoste and Carlsson, 1992; Andrady et al., 1993; La Mantia and Morreale, 2008), although Andrady (1990) and Pegram and Andrady (1989) weathered samples for a year. There is a need for greater understanding of the longer term, natural weathering of microplastics and the variables that interact in that weathering process (Tidjani, 2000). In addition, knowing how microplastic particles weather is important for understanding the ecological impacts of the most common type of marine debris.

The present study's unique results stem from longer term (i.e., 3 year) controlled exposure to natural sunlight and ambient seawater. It is therefore a more realistic proxy for the weathering processes that plastic particles experience in the open ocean than many previous studies. This is also the first study to directly compare naturally weathered plastic particles to particles collected from the ocean in an attempt to quantify the exposure time of the oceanic particles.

2. Materials and methods

2.1. Weathering experiment

Beginning in December 2010, preproduction pellets (or nurdles) of the six most common consumer plastics (Andrady, 2003) were exposed to three treatments: dry/sunlight, seawater/darkness, or seawater/sunlight, in comparison with dry/darkness control treatments. The dry/sunlight treatment roughly approximates the weathering conditions of dried plastic particles on beaches; seawater/darkness simulates conditions similar to those found in some benthic environments; seawater/sunlight simulates exposure of particles floating at the air-sea interface. The six consumer plastics were polyethylene terephthalate (PET; Resin ID #1), high density polyethylene (HDPE; Resin ID #2), polyvinyl chloride (PVC; Resin ID #3), low density polyethylene (LDPE; Resin ID #4), polypropylene (PP; Resin ID #5), and polystyrene (PS; Resin ID #6) (American Chemistry Council, 2010).

For the dry/sunlight treatment, 250 mL of each type of preproduction pellet were placed in Pyrex glass trays on the roof of Hubbs Hall at Scripps Institution of Oceanography, La Jolla, California, 32.867°N, 117.257°W. Each tray was covered by fiberglass screening (2 mm mesh size) to prevent pellet loss. Each type of plastic was placed in two trays on the roof (N = 2), except for PVC (N = 1 due to a shortage of supply pellets). The roof was covered in naturally colored pebbles, having a similar albedo effect as most beaches, and had unoccluded natural sunlight throughout daylight hours year-round.

For the seawater/darkness and seawater/sunlight treatments, 250 mL of each type of preproduction pellet were placed in 75.7 L (20 gal) aquaria with flowing seawater (N = 2 for each treatment, N = 1 for PVC). To separate plastic types, aquarium divider screens were installed. Each plastic type was randomly assigned to a location in the tank, with different locations in the two replicate tanks. Local seawater from the Scripps running seawater system (intake from the seaward end of the Scripps Pier) flowed continuously through a sprinkle bar placed over the tank, and drained through a screen-covered standpipe. The seawater/darkness treatment tanks were placed in an indoor experimental room and covered in opaque black plastic sheeting, which was only removed when the tanks were sampled. The seawater/sunlight tanks were placed side-by-side with the dry/sunlight treatments, and the tops of the aquaria were covered with fiberglass screening to prevent pellet loss.

From December 2010 to July 2012, the experiment was sampled monthly by removing ten pellets from each replicate. After July 2012, the tanks were all cleaned monthly, but the pellets were sampled bimonthly. After removal, pellets were gently wiped to remove epiphytes, rinsed with deionized water, dried at 60 °C for 24 h, and stored in glass vials in the dark at room temperature until Fourier-Transform Infrared Spectrometer (FTIR) analysis.

Seven time points were selected for analysis: T_0 = unweathered particles, T_5 = 5 months of weathering, T_9 = 9 months, T_{13} = 13 months, T_{18} = 18 months, T_{30} = 30 months, and T_{36} = 36 months. Only HDPE, LDPE and PP were analyzed for the experimental study because they are the most common plastics found at the ocean's surface, due to their common commercial use and positive buoyancy (Freund Container & Supply, 2010). In 2012, PE and PP accounted for 63% of the plastic waste in the United States (EPA, 2014).

2.2. Oceanic samples

In August 2009, samples were collected on the Scripps Environmental Accumulation of Plastic Expedition (SEAPLEX) cruise on the *R/V New Horizon* (Fig. 1). Samples were collected using a standard Manta net (0.86 m wide × 0.2 m high mouth opening) (Brown and Cheng, 1981) with 333 μm mesh, towed for 15 min at 0.7–1 m s^{-1}. Water volume flowing through the net was measured with a calibrated General Oceanics analog flowmeter. Samples were fixed in 1.8% formaldehyde buffered with sodium tetraborate.

Each sample was sorted for microplastic at 6–12 × magnification under a Wild M-5 dissecting microscope. Plastic particles were removed, dried at 60 °C, and stored in glass vials in the dark at room temperature. If there were fewer than 50 particles per sample, the entire sample was analyzed. If there were > 50 particles per sample, the sample was split using the quartering method (ASTM Standard C702/C702M-11, 2011) until an aliquot of 30–50 particles was obtained. Particles were then soaked for 12 h in 10% hydrochloric acid to remove calcium carbonate deposits, rinsed in deionized water, re-dried at 60 °C, and stored in glass vials in the dark at room temperature.

For the present study analysis, the California Current was defined as having a surface temperature < 19 °C and surface salinity < 33.5 (Lynn and Simpson, 1987). The North Pacific Subtropical Gyre (NPSG) was defined as having surface temperatures > 22 °C and salinity > 34.8 (Roden, 1980; Niiler and Reynolds, 1984). The transition region was defined as having a surface temperature of 19–22 °C and surface salinity of 33.5–34.8 (Roden, 1980; Lynn and Simpson, 1987). Because only surface data were used, these should be viewed as approximations rather than absolute oceanographic definitions

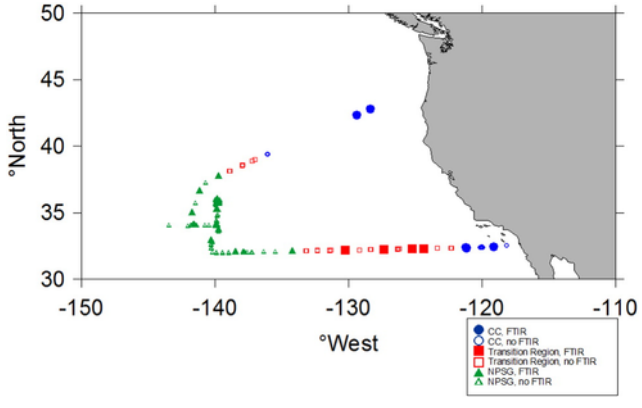

Fig. 1. SEAPLEX Manta net sampling locations. California Current (blue circles), transition region (red squares) North Pacific Subtropical Gyre (green triangles). Points indicate all locations sampled via Manta net; solid symbols are Manta samples analyzed by FTIR for this study.

(Goldstein et al., 2013). Fig. 1 reflects the sampling locations of the SEAPLEX cruise, with filled shapes indicating those sampling stations analyzed using FTIR in this study. These stations were chosen so that they were distributed throughout the cruise track, without reference to the abundance of plastic in each sample. Median bond indices (see below) from the three regions were compared by the Kruskal-Wallis test, then a multiple comparison test performed, adapted from Siegel and Castellan (1988), where significance between two regions was defined as $p < 0.05$.

2.3. FTIR

Both ocean-collected and weathering experiment samples were analyzed using a Fourier-Transform Infrared Spectrometer with an attenuated total reflectance (ATR) diamond crystal attachment (Nicolet 6700 with Smart-iTR). All spectra were recorded at 4 cm^{-1} resolution. The FTIR spectra for particles collected from the ocean were compared to both published standards (Forrest et al., 2007) and in-house standards for the 6 common consumer plastic types listed above. LDPE was distinguished from HDPE by the presence of a peak at 1377 cm^{-1}, with its presence indicating LDPE and absence HDPE (Fig. 2) (Lobo and Bonilla, 2003). If the type of polyethylene could not be positively determined, the sample was classified as unknown PE, which occurred in 30% of oceanic polyethylene samples.

For experimental weathering samples, 5 particles were randomly subsampled from the 10 particles collected at each time point. Depending on particle shape, either 2 or 3 spectra were obtained from different locations on each particle. For asymmetrical particles, especially LDPE which were often concave discs, the location of the spectra reading on the particle was determined to affect values due to the need for precise contact with the ATR crystal (Gulmine et al., 2002). Particles only demonstrated clean readings if the ATR crystal was completely, or almost completely, covered in plastic, and there was no trapped air between the plastic particle and the crystal. Clean spectra from different regions of a single particle were treated as independent and averaged. If a particle split into pieces or crumbled into powder while performing FTIR, readings of both the inside and outside of the pieces were taken and treated as independent, if readings were distinct.

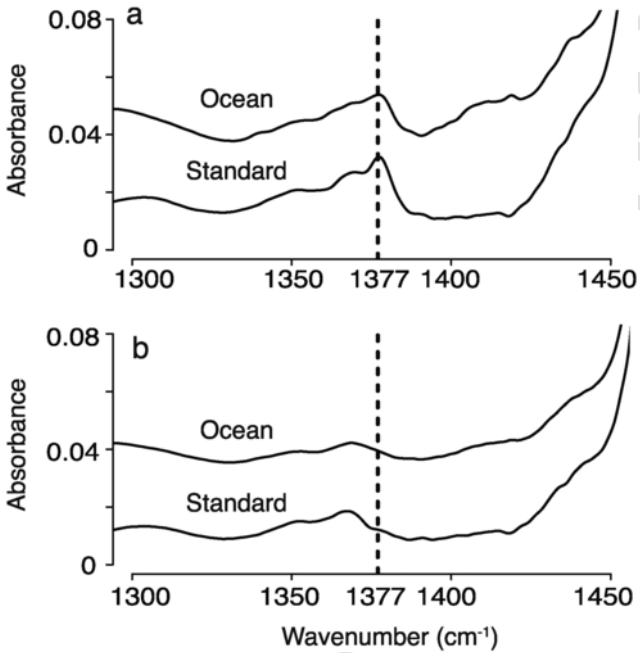

Fig. 2. Portion of FTIR spectra of microplastics collected from the ocean compared to laboratory standards. a) Low-density polyethylene (LDPE) and b) high-density polyethylene (HDPE).

Three likely areas of weathering-related change in infrared spectra were first identified from previous research: hydroxyl groups (broad peaks from 3100 to 3700, centered at 3300–3400 cm^{-1}), alkenes, or carbon double bonds (1600–1680 cm^{-1}), and carbonyls (1690–1810 cm^{-1}, centered at 1715 cm^{-1}) (Albertsson et al., 1987; Lacoste and Carlsson, 1992; Socrates, 2004; Pavia et al., 2008; Rajakumar et al., 2009). The hydroxyl peaks in our spectra had the broad peak shape and location of intermolecular hydrogen bonded O—H bonds (Socrates, 2004; Pavia et al., 2008). When carbon double bonds are non-conjugated in a hydrocarbon, they are often seen from 1620 to 1680 cm^{-1}, and at lower frequencies, around 1600 cm^{-1} if conjugated; however symmetrically substituted bonds are often IR inactive (Socrates, 2004; Pavia et al., 2008). Carbonyl bonds have a strong IR signal and appear in a wide range of wavelengths, even as wide as 1550–1850 cm^{-1} (Socrates, 2004), and so the frequency of a ketone, 1715 cm^{-1}, is often used as the central reference for the range of these values (Pavia et al., 2008).

Three additional areas of change in the plastics' spectra, 1000–1200 cm^{-1}, 1200–1280 cm^{-1}, and 1540 cm^{-1}, were located empirically. The peak at 1540 cm^{-1} was very close to the 1640 cm^{-1} peak and the commonly cited peak for changes in carbonyl bonds (1715 cm^{-1}) (Lacoste and Carlsson, 1992) also often overlapped with the peak centered at 1640 cm^{-1}. The IR signal for double bonds is weaker than that for carbonyl bonds, the bonds are in overlapping ranges, and symmetrically substituted double bonds are inactive. Due to all of these factors, the entire range of 1550–1810 cm^{-1} was referred to as the "carbonyl groups." All carbonyl groups are indicative of oxidized carbon in the plastic hydrocarbon chain, and were grouped together throughout the manuscript. This manuscript is less concerned with which specific carbonyl group is present, but rather with whether plastic has oxidized as it has weathered, and the presence of carbonyls show that oxygen has bonded with the hydrocarbon chain.

The empirically located region at 1000–1200 cm^{-1} is the spectral range of carbon-oxygen bonds and 1200–1280 cm^{-1} is the range of carbon-nitrogen bond stretching in secondary amines (El-Ghaffar et al., 1998; Pavia et al., 2008). Although pure PE and PP do not have any nitrogen in their structure, nitrogen is the main component in air and is present in seawater, and can be found in plastic additives; C—N bonds have been measured on plastics via X-ray photoelectron spectroscopy (Stark and Matuana, 2004). However, these results were not considered further because C—N bonds are unlikely to be seen in large quantities in plastics, and because their peak was weak in our spectra and changed little over time. The commonly cited peak for changes in vinyl groups (centered around 909 cm^{-1}) (Tidjani, 2000) was also too weak in our spectra to be read accurately.

Indices of hydroxyl, carbon-oxygen bonds, and carbonyl group bonds were calculated as the ratio of the maximum absorbance value for the bond peak relative to the value of a reference peak. Several reference peaks have been used previously, including 974 cm^{-1} and 2720 cm^{-1} for PP (Livanova and Zaikov, 1992; Rabello and White, 1997; Rajakumar et al., 2009) and 1465 cm^{-1} and 2020 cm^{-1} for PE (Albertsson et al., 1987; Roy et al., 2011). We selected 2910 cm^{-1} for PE and 2920 cm^{-1} for PP because these peaks, both also characteristic of plastic type, are thought to change little with weathering, as corroborated in our study (Socrates, 2004).

Bond indices were therefore calculated as the ratio of the maximum peak absorbance (numerator) to the value of a reference peak (denominator) as follows (Table 1): hydroxyl (LDPE/HDPE 3300–3400 cm^{-1}/2908–2920 cm^{-1}; PP 3300–3400 cm^{-1}/2885–2940 cm^{-1}), carbonyl groups (LDPE/HDPE 1550–1810 cm^{-1}/2908–2920 cm^{-1}; PP 1550–1810 cm^{-1}/2885–2940 cm^{-1}), and carbon-oxygen (LDPE/HDPE 1000–1200 cm^{-1}/2908–2920 cm^{-1}; PP 1000–1200 cm^{-1}/2885–2940 cm^{-1}).

Before calculating indices, baselines were corrected using Essential FTIR/eFTIR software (http://www.essentialftir.com). All spectra were corrected using eFTIR's Advanced ATR (Attenuated Total Reflectance) Correction that used the Refractive Index (RI) of each plastic type, thickness of each particle, and the Angle of Incidence to correct for dispersion and depth of penetration. The parameters used were: RI: 1.57 for PS, 1.5 for PE, 1.49 for PP, 1.65 for PVC, and 1.5 for PET (Samuels, 1981; Markelz et al., 2000; Ma et al., 2003; Rodriguez-Gonzalez et al., 2003; Piesiewicz et al., 2007); thicknesses: 0.2 cm for PS, 0.2 cm for PE, 0.3 cm for PP, 0.5 cm for PVC, and 0.2 cm for PET; angle of incidence: 42°. The samples were then corrected by normalizing to a minimum of zero and the maximum absorption value of each spectrum (Workman and Springsteen, 1998).

After ATR correction and normalization of the baseline, spectra were excluded that were too low, in order to remove any samples of extremely low signal-to-noise ratio. Samples were also removed that had very jagged or blocky spectral baselines, that did not have flat baselines even after normalization, or that did not have clear definition between the hydroxyl peak and the C—H reference peak at 2910 cm^{-1}. The precision of the plastic placement on the ATR crystal, the humidity of the FTIR analysis room, and the operator of the instrument could all add variability to the spectral readings.

2.4. Brittleness-crystallinity

Crystallinity was calculated by the method used in Zerbi et al. (1989) and Stark and Matuana (2004). Doublet peaks at 730 and 720 cm^{-1} correspond to polyethylene crystalline content (730 cm^{-1}) and amorphous content (720 cm^{-1}) (Zerbi et al., 1989; Stark and Matuana, 2004); 841 cm^{-1} corresponds to polypropylene crystalline content and 1170 cm^{-1} corresponds to polypropylene amorphous content (Tadokoro et al., 1965; Livanova and Zaikov, 1992).

The percentage crystalline content was calculated from:

$$X = 100 - \frac{(1 - I_c/I_a)/1.233}{1 + I_c/I_a}(100)$$

where I_c is the band at 730 cm^{-1} or 841 cm^{-1} and I_a is the band at 720 cm^{-1} or 1170 cm^{-1} and 1.233 relates to the theoretical intensity ratio for I_c/I_a at setting angle 42° (Avitabile et al., 1975; Abbate et al., 1979; Zerbi et al., 1989; Stark and Matuana, 2004).

Table 1
Wavenumbers used to measure weathering in FTIR spectroscopy.
The numerators of the bond indices are the same for PE and PP, but the reference peaks/denominators differ. The peaks used were centered in the ranges given below, with some variability among samples.

	Hydroxyl	Carbonyl groups	Carbon-oxygen
PE numerator	3300–3400[a]	1550–1810[b]	1000–1200[a]
PE denominator	2908–2920[c]	2908–2920[c]	2908–2920[c]
PP numerator	3300–3400[a]	1550–1810[b]	1000–1200[a]
PP denominator	2885–2940[c]	2885–2940[c]	2885–2940[c]

[a] Pavia et al. (2008).
[b] Corrales et al. (2002).
[c] Socrates (2004).

2.5. Temperature

Elevated temperatures can accelerate aging of plastics (Lacoste and Carlsson, 1992; Stark and Matuana, 2004), so the temperature of the experimental conditions was recorded as follows. Sunlight samples were assumed to weather at the ambient air temperature of La Jolla, CA, obtained from NOAA's National Data Buoy Center Water Level Observation Network (http://www.ndbc.noaa.gov/). Air temperature was measured at Station LJAC1 (9410230) on the Scripps Pier at 32.867° N, 117.257° W at 16.46 m above sea level. NOAA measurements were recorded every 6 min, but here data were averaged every 8 h. For the seawater/darkness treatment, which used running seawater from the Scripps Pier, the seawater temperature was assumed to be the same as the seawater temperature recorded at NOAA Station LJAC1, at a depth of 3.44 m below sea level, also recorded every 6 min and averaged every 8 h.

To test for a difference in temperature between the seawater/sunlight tanks and the NOAA pier readings, in April 2014, HOBO Water Temp Pro v2 data loggers were placed in the seawater/sunlight tanks, recording temperature every 60 min. A HOBO logger was placed in both of the seawater/sunlight treatment tanks, and temperature recordings averaged every 8 h.

3. Results

3.1. Temperature

Air temperatures at the Scripps Pier varied between 5.9 and 30.4 °C and seawater temperatures near the Scripps Pier varied between 14.6 and 18.3 °C over the course of the plastics weathering experiment, with clear seasonal variation and a slight upward trend (Fig. 3). Data loggers placed in the pellet weathering tanks showed that the experimental tank temperatures averaged 2.7 °C greater than pier seawater, but followed the seasonal trends closely.

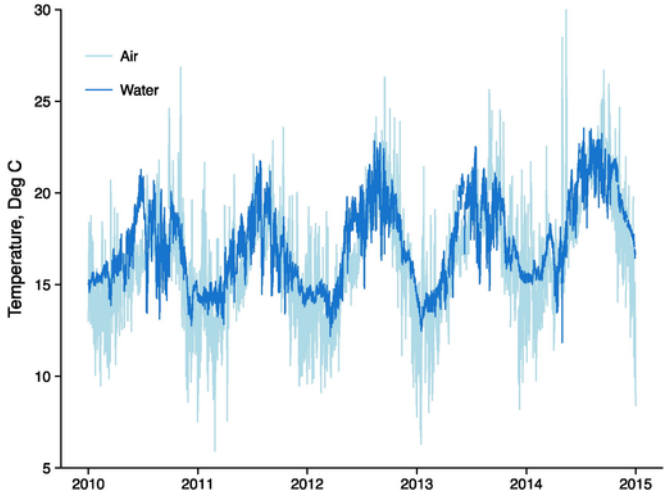

Fig. 3. Temperature. Ambient air temperature from NOAA's National Data Buoy Center's Station LJAC1 on the Scripps Pier (light blue) and ambient seawater temperature from Station LJAC1 (dark blue). (For interpretation of the references to color in this figure legend, the reader is referred to the web version of this article.)

3.2. Experimental weathering

There were clear changes in chemical bond structure with weathering (Fig. 4), as evidenced by the difference in height between the unweathered HDPE (T_0) (gray line), and the HDPE from the seawater/darkness treatment after 36 months (blue line).

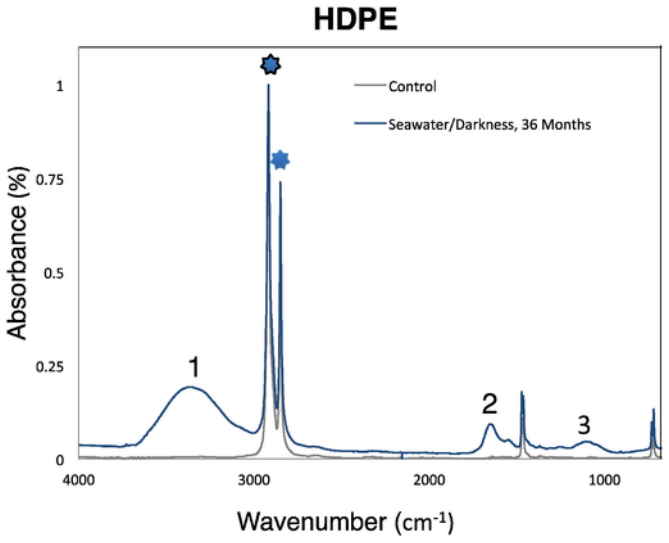

Fig. 4. FTIR spectrogram. Unweathered HDPE at T_0 (gray) and weathered HDPE at 36 months from the seawater/darkness treatment (blue). The changes in bond height at 3350 cm^{-1} (hydroxyl), 1640 cm^{-1} (carbonyl groups), and 1070 cm^{-1} (carbon-oxygen) are indicated by the numerals 1–3, respectively. The blue symbols near 2910 cm^{-1} and 2848 cm^{-1} indicates diagnostic PE doublet peaks, with the black outlined symbol at 2910 cm^{-1} also indicating the reference peak for PE weathering. (For interpretation of the references to color in this figure legend, the reader is referred to the web version of this article.)

For the weathering experiment, we first describe results from the seawater/sunlight treatment, as this best simulates the conditions experienced by particles suspended in seawater in open ocean conditions. We then describe the effects of exposure to seawater/darkness and dry/sunlight for comparison.

Fig. 5 illustrates the seawater/sunlight treatment (pink) in relation to the control treatment of dry/darkness intended to induce the least amount of environmentally-induced weathering (gray; cf. Hidalgo-Ruz et al., 2012). For all three bonds, across all three plastic types, the control barely changed between 0 and 36 months. In contrast, exposure to seawater/sunlight resulted in time-dependent changes in hydroxyl bonds (Fig. 5a–c). For PE, there was a general increase in this bond index to 13 months, then a decrease at 18 months that lasted until 30 months, where it began to increase again. For PP, the same pattern was evident, but with a transient dip at 9 months, and no increase from 30 to 36 months.

Carbonyl groups (Fig. 5d–f) and carbon-oxygen bonds (Fig. 5g–i) show similar temporal patterns to the changes in hydroxyl groups for all three plastic types, with an increase from 0 to 13 months, a decrease between 13 and 30 months, and for PE, another increase from 30 to 36 months. LDPE had the steepest decrease from 13 to 30 months. The magnitude of the change in all PP bonds was substantially larger than the changes in these bonds for either LDPE or HDPE.

Turning to the other weathering treatments, Fig. 5 illustrates that for PE, there was a significant difference between the seawater/sunlight and dry/sunlight treatment at multiple time points ($p < 0.05$, based on non-overlapping confidence limits). There was a significant difference between seawater/sunlight and dry/sunlight treatments for LDPE at 13 months for hydroxyl, 9 and 30 months for carbonyl

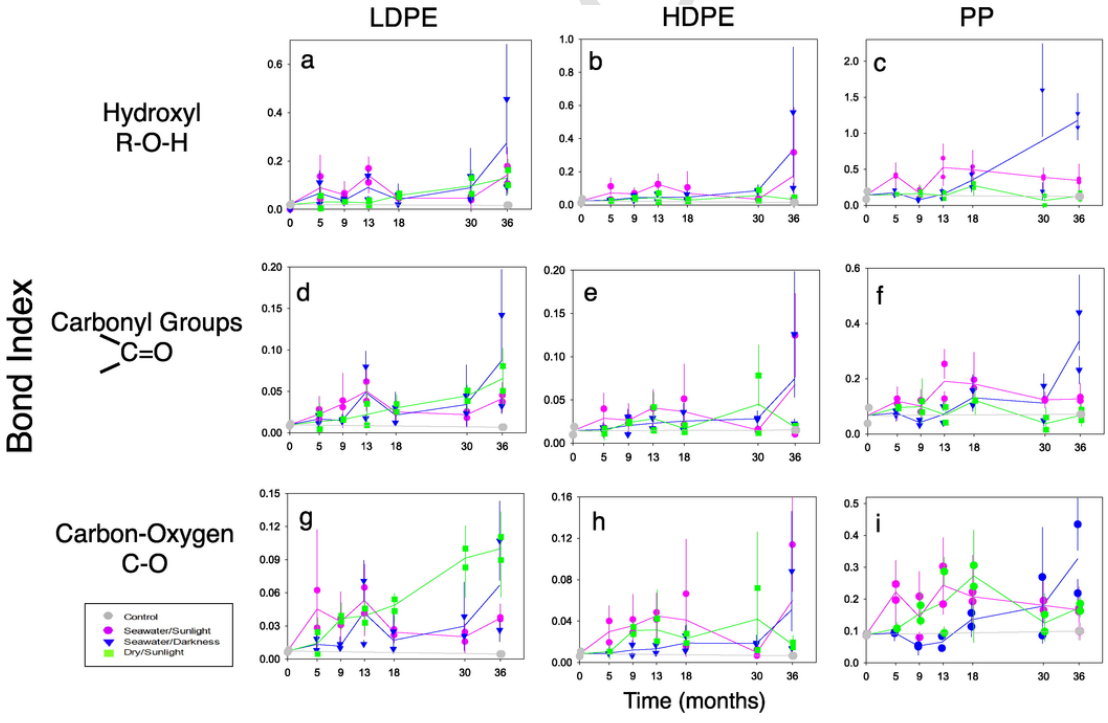

Fig. 5. Experimentally weathered LDPE, HDPE, and PP. FTIR results from experimentally weathered (a, d, g) LDPE, (b, e, h) HDPE, and (c, f, i) PP, for (top row) hydroxyl bonds, (middle row) carbonyl groups, and (bottom row) carbon-oxygen bonds. Seawater/sunlight experimental treatment (pink); dry/sunlight (green); seawater/darkness (blue); control of dry/darkness (gray). The two dots at each treatment represent means of the two separate tanks. Error bars indicate 95% confidence intervals.

groups, and 18 months onward for carbon-oxygen. For HDPE, there was only a significant difference at 5 and 36 months for carbon-oxygen. In contrast, for PP, there were significant differences between the seawater/sunlight and dry/sunlight treatments at most time points for hydroxyl and carbonyl groups, though none for carbon-oxygen. Comparing seawater/sunlight and seawater/darkness treatments for PE, there was no significant difference between treatments until 36 months; at T_{36} for many of the bonds one of the two replicates of seawater/darkness had the highest values, though the average of the two replicates was not significantly higher than seawater/sunlight. This contrast also holds for T_{30} for PP hydroxyl. For PP hydroxyl bonds and carbonyl group bonds, the seawater/darkness values were significantly higher at 36 months than the seawater/sunlight values ($p < 0.05$).

Despite the lack of consistent differences between seawater/sunlight and the other treatments, the shapes of the weathering curves of the other two treatments appear somewhat different than seawater/sunlight. Dry/sunlight treatments show a quasi-linear change with time for all LDPE bonds. Seawater/darkness treatments show a much steeper increase from 30 to 36 months across all treatments. For LDPE carbon-oxygen bonds, seawater/darkness does not show the same initial increase at 9 months as seawater/sunlight; but after 13 months the values closely mirror seawater/sunlight until the steeper increase from 30 to 36 months. For HDPE and PP carbon-oxygen, the three treatments show somewhat different temporal progressions.

3.3. Oceanic particles

Fig. 6 compares experimental HDPE particles exposed to sunlight/seawater, and the corresponding control treatment, with oceanic HDPE particles from the North Pacific Subtropical Gyre (NPSG, dark gray histograms), transition region (TR, light gray histograms), and the California Current (CC, white histograms). Oceanic particles that could only be assigned to PE (but not to high or low density polyethylene) are compared to experimental results from both LDPE and HDPE in Supplemental Figs. 1 and 2 (discussed below).

Nearly all HDPE particles from all three oceanic regions are within the range of experimental determinations. Values from the three regions typically overlap both the 0–9 month and 18–36 experimental determinations. There is no significant difference among oceanic regions for hydroxyl bonds or carbon-oxygen bonds ($p > 0.05$); for carbonyl groups, the NPSG (dark gray, Fig. 6) and CC (white, Fig. 6) samples differ ($p < 0.05$) but neither is significantly different from the transition region.

For LDPE (Fig. 7), the majority of the oceanic values for all three bonds are within the range of the experimental values, although many exceed the range measured in the laboratory. Thirty percent of the values from the NPSG (dark gray, Fig. 7) are very low, corresponding to either the 0–9 month or 18–30 month experimental values for hydroxyl, with the next 28% corresponding with 30–36 months. For carbonyl, over 50% of the oceanic values correspond with 0–9 or 18–30 month values. For carbon-oxygen, 24% of the values are low, corresponding with 18–30 months. Values from the more nearshore California Current samples (white, Fig. 7) are variable, with a low mode for all three bonds, although sample sizes were small. Values for the transition region samples exceed most of the experimental values for hydroxyl and carbon-oxygen. For hydroxyl and carbon-oxygen bonds, there is a significant difference between the California Current and the transition region samples, and the transition region and the NPSG ($p < 0.05$, Kruskal-Wallis with multiple comparisons test). For carbonyl groups, there is no significant difference among the three oceanic regions ($p > 0.05$) and the majority of all values for all three regions are within the range of experimental values.

In Supplemental Fig. 1, some of the highest NPSG values only overlap the high experimental data point and 95% confidence interval for 36 months. Values from the three regions typically overlap both the 0–9 month and 18–36 experimental determinations. There is no significant difference among all three oceanic regions for any of the three bonds. In Supplemental Fig. 2, we compare the same undifferentiated oceanic PE plastic as Supp. Fig. 1 with experimentally weathered LDPE. The majority of the oceanic values for all three bonds are within the range of the experimental values, although many exceed the range measured in the laboratory. Most of the NPSG samples (dark gray) are low, overlapping with 0–9 months or 18–30 month samples, with the transition region samples being slightly higher. There is no significant difference among all three oceanic regions for any of the three bonds.

Fig. 8 compares experimental PP particles exposed to seawater/sunlight and the corresponding control treatment with ocean-collected PP particles. There is little overlap between the experimental values and the oceanic values, suggesting the bonds used here are not useful for quantifying the exposure time of PP plastic. There is more

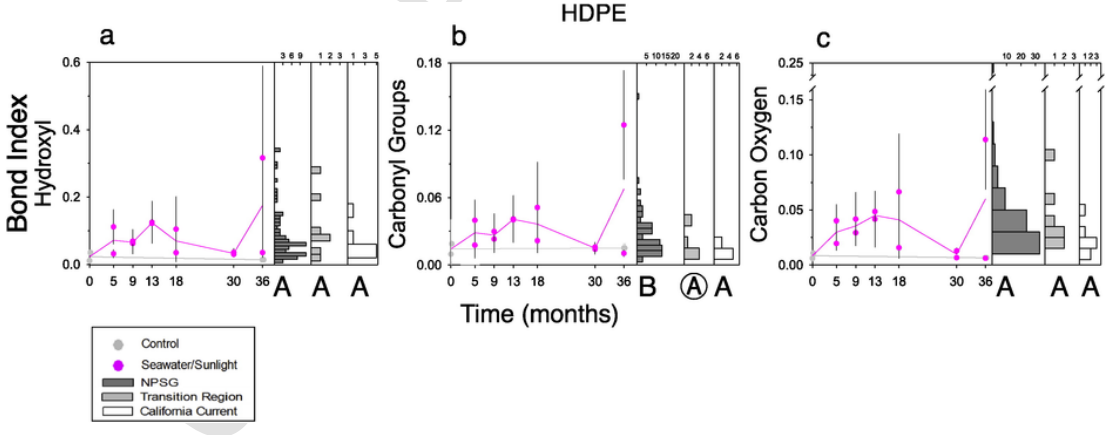

Fig. 6. Experimentally weathered HDPE compared to oceanic HDPE. FTIR results from experimentally weathered HDPE (pink lines) compared to oceanic HDPE particles (histograms), for (a) hydroxyl bonds, (b) carbonyl groups, and (c) carbon-oxygen bonds. Seawater/sunlight experimental treatment (pink line); control of dry/darkness (gray line). The two dots at each treatment represent means of the two separate tanks. Error bars indicate 95% confidence intervals. Histograms are SEAPLEX samples: North Pacific Subtropical Gyre (dark gray), transition region (light gray), California Current (white). The capital letters indicate regions that differ ($p < 0.05$) in a multiple comparisons test. A and B differ, Ⓐ differs from neither. (For interpretation of the references to color in this figure legend, the reader is referred to the web version of this article.)

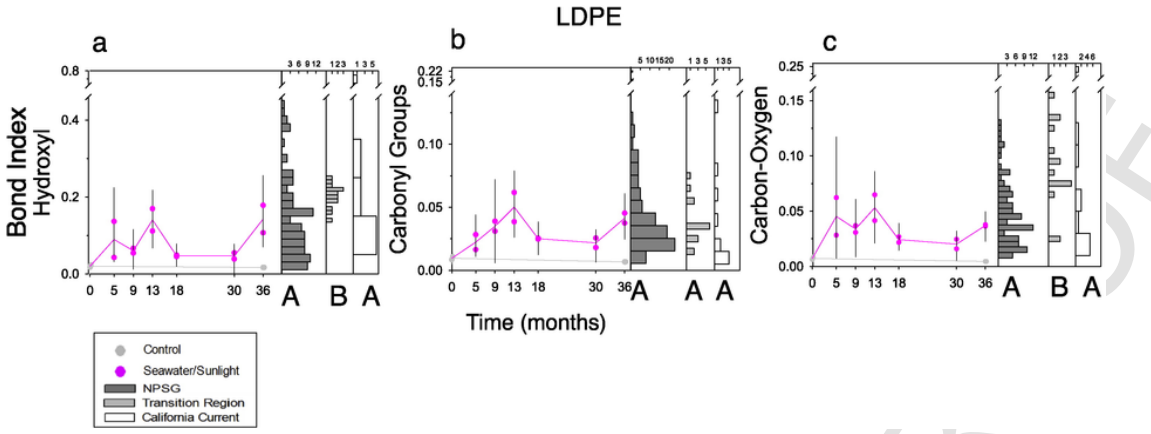

Fig. 7. Experimentally weathered LDPE compared to oceanic LDPE. FTIR results from experimentally weathered LDPE (pink lines) compared to oceanic LDPE particles (histograms), for (a) hydroxyl bonds, (b) carbonyl groups, and (c) carbon-oxygen bonds. Seawater/sunlight experimental treatment (pink line); control of dry/darkness (gray line). The two dots at each treatment represent means of the two separate tanks. Error bars indicate 95% confidence intervals. Histograms are SEAPLEX samples: North Pacific Subtropical Gyre (dark gray), transition region (light gray), California Current (white). The capital letters indicate regions that differ ($p < 0.05$) in a multiple comparisons test. A and B differ, Ⓐ differs from neither. (For interpretation of the references to color in this figure legend, the reader is referred to the web version of this article.)

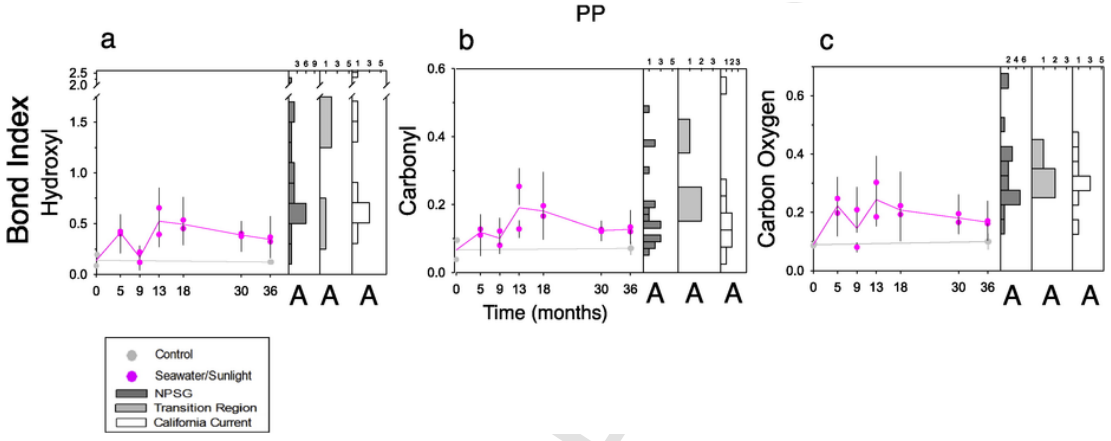

Fig. 8. Experimentally weathered PP compared to oceanic PP. FTIR results from experimentally weathered PP (pink lines) compared to oceanic PP particles (histograms), for (a) hydroxyl bonds, (b) carbonyl groups, and (c) carbon-oxygen bonds. Seawater/sunlight experimental treatment (pink line); control of dry/darkness (gray line). The two dots at each treatment represent means of the two separate tanks. Error bars indicate 95% confidence intervals. Histograms are SEAPLEX samples: North Pacific Subtropical Gyre (dark gray), transition region (light gray), California Current (white). The capital letters indicate regions that differ ($p < 0.05$) in a multiple comparisons test. A and B differ, Ⓐ differs from neither. (For interpretation of the references to color in this figure legend, the reader is referred to the web version of this article.)

overlap between experimental and oceanic carbonyl group values than the other two bonds. None of the oceanic regions differ significantly from each other ($p > 0.05$).

3.4. Crystallinity

In both PE and PP, there were only slight differences in crystallinity over time, and a large range of values at every time point except the control. Crystallinity, as measured in Zerbi et al. (1989) and Stark and Matuana (2004), was not found to be a useful metric of aging in the present experiment, and the results are not discussed further here.

3.5. Qualitative observations of yellowness, opacity, and brittleness

There was clear visual evidence of an increase in opacity and yellowness in all experimental samples as time increased. When comparing all six types of consumer plastic tested in this experiment, the plastics that yellowed most were polystyrene (PS) and polyvinyl chloride (PVC). For LDPE, HDPE, and PP, by 36 months the sunlight treatment of both PP and LDPE were turning yellow, although the larger change in all three of these plastic types was in opacity and brittleness. A slight change in opacity could be seen in all of these plastics by 9 months, with clear, translucent PP and white-tinged, glossy HDPE turning fully opaque and dull in the sunlight treatment by 30 months.

Qualitatively, increased brittleness was detected as the experiment progressed. Pellets became more brittle with duration of environmental exposure, with PP becoming the most brittle of the three main plastics examined. By 9 months, HDPE and PP pellets (dry/sunlight treatment) would splinter and split into large pieces under the pressure of the FTIR stabilizing arm, while LDPE was still malleable. By 18 months, the dry/sunlight LDPE samples would flatten and break under the pressure. By 30 months, LDPE seawater/darkness samples were still malleable, but the seawater/sunlight samples would flatten under the pressure of the FTIR stabilizing arm and never regain their shape. By 30 months PP and HDPE dry/sunlight samples would often

crumble into powder. At 36 months, both PP and LDPE sunlight/seawater samples broke into small pieces as well.

4. Discussion

FTIR is a useful method to differentiate among the most common types of buoyant plastics that are found at the sea surface. We distinguished polypropylene (PP) from polyethylene (PE) in 100% of the ocean-collected particles analyzed. We could differentiate low density polyethylene (LDPE) from high density polyethylene (HDPE) in 70% of the particles. Some of the 30% that could not be distinguished may have been a manufactured PE blend or LLDPE (linear low density polyethylene), which is a rare plastic that we did not test.

Numerous other studies have utilized FTIR spectroscopy to identify marine debris in sediments (Thompson et al., 2004; Reddy et al., 2006; Frias et al., 2010) as well as to identify ingested plastic (Eriksson and Burton, 2003), but the present study appears to be one of the first to identify suspended sea surface marine debris particles with FTIR (Rios et al., 2007). That small fragments whose original purpose and provenance can no longer be identified can nevertheless be sorted to plastic type demonstrates that FTIR is useful for marine debris research. It is more accurate than the buoyancy method often used (Hidalgo-Ruz et al., 2012).

Ioakeimidis et al. (2016) also used FTIR spectroscopy to determine the exposure time of plastic marine debris, though they looked at PET plastic bottles. They also observed plastic change its chemical bond structure with weathering, measuring bonds that had never been documented in PET before. They highlight the need for a laboratory weathering study with which to properly compare their environmental results, which is the aim of this present study.

The bond indices presented here (hydroxyl, carbonyl groups, carbon-oxygen) may be most useful in future work quantifying the exposure time of PE, especially HDPE, from the field, due to the overlap in values in experimental and oceanic PE values. The bonds measured here for experimental weathering changes in PP do not apply well to oceanic PP samples. This may be because the experimental weathering was performed on pure pre-production PP, and the oceanic PP, with colorants and additives, may have reacted differently to environmental exposure.

It would be advisable to carry out weathering experiments for a longer duration than the 36 months considered here, to determine whether the observed nonlinear aging patterns continue their upward trajectory after 36 months or dip again. It would also be advisable because floating particles may circulate in gyres indefinitely (Maximenko et al., 2012) and chemical bonds may therefore change substantially in comparison with what we have observed. The increasing PE bond measures from 30 to 36 months and the oceanic samples that are higher than any experimentally recorded values also suggest that an experiment of longer duration than 36 months could be useful. The timeline of 36 months may have been appropriate for comparison for HDPE, as evidenced by the vast majority of the oceanic and experimental particles overlapping, but for LDPE a longer duration experiment may be useful.

The hydroxyl peak was the most readily identified on the spectrograms, followed by the carbon-oxygen peak. The packet of carbonyl groups was less distinctive. Overall, hydroxyl was the most useful index because of ease of identification on spectrograms and the overlap in magnitude of the experimental and oceanic plastics. Carbonyl groups had the next greatest degree of overlap in naturally and experimentally weathered particles.

Although Carlsson et al. (1985) and Lacoste and Carlsson (1992) state that oxidized plastic polymers are always unstable at room temperature in the dark, and should be stored at − 30 °C to limit continued slow oxidation, they base this recommendation on Carlsson et al.'s aging experiment with PP exposed to gamma irradiation. In contrast, our experiment, with natural radiance including UV wavelengths, exhibited stable baselines in the controls.

4.1. Nonlinearity of results

Almost all the experimental samples returned to near-T_0 levels of bond index values at some time during the experiment, which introduces some ambiguity in attempting to quantify the exposure time of naturally weathering plastics. HDPE showed a decline to near-T_0 levels at 30 months and LDPE from 18 to 30 months. This nonlinearity could be due to many factors, but one possibility is that the observed "reverse weathering" may actually have been due to the brittleness of the plastic, thus exposing newer, less weathered interior plastic over time. This brittleness hypothesis is discussed below in detail. However, we are still left with nonlinear experimental results to compare to oceanic samples, and it is highly unlikely that the open ocean samples are of new plastic close to weathering duration of 0. Most are likely to be older samples that have weathered for 12 months or more in the ocean environment.

It is also difficult to estimate the apparent age of the oceanic plastics because a piece of plastic may have been manufactured decades earlier but been protected from weathering until it entered the ocean, or it could have aged for years in direct sunlight on a beach before entering the California Current. FTIR thus can only give a rough approximation of exposure time, not true age. However, it still is a useful method for comparison between experimental and naturally weathered particles.

Due to the likely continental source regions of most plastic particles and their different residence times in different ocean circulation features, the North Pacific Subtropical Gyre, transition region, and California Current would be expected to contain suspended plastics of different exposure times. Models of gyre circulation indicate that particles spend different amounts of time in the three provinces analyzed here (Kubota, 1994; Maximenko et al., 2012). Most of the plastic in the ocean is thought to enter from the coasts and be transported into the gyres, although there is likely some lesser amount of direct plastic disposal from ships into the gyres (Kubota, 1994, Ocean Conservancy, 2010), particularly in the years before 1989, when the International Marine Organization's MARPOL Annex V prohibited all plastic disposal at sea by all classes of ships. If the primary source of plastics in this region were continental sources along the west coast of North America into the California Current, followed by transport of particles southward and westward into the transition region, and finally into the NPSG, the exposure times of particles would be expected, on average, to follow this progression. Our oceanic LDPE samples agree with this inference, where there is a significant difference between NPSG and California Current and NPSG and transition region samples for hydroxyl and carbon-oxygen. That the California Current and NPSG samples do not differ is consistent with the nonlinear experimental results. If the CC samples were exposed for less time (0–13 months), the transition region samples intermediate (around 13 months), and NPSG samples exposed for a longer duration (18–36 months), then the California Current and NPSG bond indices should have similar medians and the transition region should have a higher one. Often with the NPSG plastic samples, some qualitative characteristics of brittleness, opacity, or presence of a biofilm helped reinforce this inference of progressive exposure time from the coast to the open ocean. For HDPE, only the CC and NPSG samples significantly varied for carbonyl, and none of the other bonds varied for the oceanic regions.

We expect, according to ocean circulation models, that the majority of NPSG samples would be at least 5 years old, and not younger than 12 months (Kubota, 1994; Maximenko et al., 2012). It takes one year for modeled debris to begin converging into the NPSG (Dotson et al., 1977; Kubota et al., 2005; Maximenko et al., 2012), and the majority of the modeled debris is not only still there, but more concentrated, five to ten years later (Kubota, 1994; Maximenko et al., 2012). The majority of our NPSG PE values are consistent with the experimental values of 13 months or more, with most being consistent with 30 months or more. Results from PP did not permit age approximation.

It is possible that the PE and PP in the ocean are themselves different "ages". Such differences could arise due to differences in input amounts and locations, slight differences in buoyancy (0.89–0.91 g/cm^3 for PP, 0.94–0.965 g/cm^3 for HDPE) (Freund Container & Supply, 2010) and the way in which they weather in the ocean. The SEAPLEX samples from the California Current were comprised of 49% PP particles, but that decreased to only 12% in the NPSG; in the NPSG 86% of the particles tested were PE. This contrast shows that there can be regional differences in distributions of plastic types in the ocean. However, it is also possible that PP samples weather and degrade to pieces smaller than 333 μm, and are thus present in the NPSG but were missed by nets used in this study.

These oceanic distribution numbers also treat PE as one plastic. LDPE and HDPE are used for different consumer products and have vastly differently recycling rates (74% for HDPE versus 2% for LDPE in California in 2015) (CalRecycle, 2016) and our experimental results indicate they weather differently under different conditions. It is essential to be able to spectrally distinguish LDPE from HDPE, as we were able to do in 70% of our oceanic samples, in order to better distinguish inputs of marine debris, how debris is traveling in the ocean, and how each of the most common plastics, PP, LDPE, and HDPE, are degrading in the water column.

4.2. Yellowness, opacity, and brittleness

The nonlinearity of bond measures could be due to many factors, but one possibility is that it demonstrates the complexity in measuring the exposure time of brittle, weathered plastic: the more brittle plastic gets, the more likely it is that it will break and expose the newer, less weathered plastic at its interior.

As discussed, the pellets became very brittle around 9 months, and often split open (PP and HDPE dry/sunlight samples by 9 months, all three plastics dry/sunlight samples by 18 months). Thus what may appear like plastic "reverse weathering" as a bond index decreases may have actually been a result of sampling less exposed plastic in the interior of the particles. Because plastic weathers from the outside, a split pellet would reveal less environmentally exposed plastic on the particle interior. Similarly, pellets that crumbled into powder (ex. HDPE and PP dry/sunlight by 30 months) would have less exposed plastic on the inside that was measured when the powder was sampled. This could explain the decrease from 18 to 30 months in PP and HDPE and low value at 30 months for LDPE. The subsequent increase by 36 months could occur as the plastic weathered so thoroughly that the effect of a split pellet or powdered pellet did not affect analytical results. This brittleness hypothesis may also explain why so many oceanic samples are higher than experimental samples. If those samples were taken from larger pieces of plastic, they would have less tendency to crumble, and thus may be giving a more accurate measure of changes in bond structures. In contrast, the small nurdles used in this experiment may have been small enough that their cores always became brittle before reaching high index values.

Jabarin and Lofgren (1994) naturally weathered sheets of HDPE in sunlight. They observed increased embrittlement, decreased elongation to break (the amount the sheets could be stretched before breakage or crack formation), increased crystallinity, and decreased molecular weight due to environmental degradation. Although elongation to break can only be measured on long pieces like the plastic sheets they measured, and we did not measure molecular weight, we also saw increased brittleness and loss of ductility, and our results of the effects of natural sunlight on PE agree with their findings. Although our crystallinity results were inconclusive, we observed an increase in brittleness, and brittleness has been associated with an increase in crystallinity (Jabarin and Lofgren, 1994).

Stark and Matuana (2004) exposed plastic samples to xenon light and water for 12 min of every 120. They detected near-immediate surface oxidation of their samples and increased oxidation with time. There was an increase in the ratio of oxidized to unoxidized carbons with continued weathering, and an increase in the elemental ratio of oxygen to carbon. Stark and Matuana (2004) noted that the increase in oxidized: unoxidized carbon appears to be mainly from an increase in hydroxyls, which would explain our short-term increase in hydroxyls as well since hydroxyls form in response to surface oxidation of the plastics. This surface oxidation would also explain the formation of C—O bonds (cf. Stark and Matuana, 2004). Stark and Matuana (2004) stated that oxidative degradation is the main limiting factor on the "active life of synthetic polymers" and that those oxidative degradation reactions are accelerated by UV radiation, which agrees with our carbon-oxygen bonds showing higher values for the two natural sunlight treatments for almost all time points and all three plastics.

Polypropylene has been observed to become brittle on beaches before ever entering the ocean, and its weathering is known to slow once in seawater (Andrady, 2011). The more pronounced temporal changes that we detected in PP relative to the other two plastic types can perhaps be attributed to such a reduction in brittleness in an aqueous medium.

5. Conclusions

We found FTIR to be a useful method to differentiate among the most common buoyant marine microplastic particle types (especially PP, LDPE, and HDPE) that are found suspended in the upper ocean.

The experimental weathering was more complex than predicted; the chemical bonds did not change linearly with time, and there was variability in weathering between the combinations of plastic, weathering experiment, and bond type measured. Due to the nonlinear changes in bond indices with experimental weathering, the indices presented here are of potential use for quantifying the exposure time of plastics only over a relatively limited time period, generally for differentiating younger (0–18 months) from older (> 18–30 months) particles. These experimental results are based on pure pre-production plastic pellets, and their applicability to more complex manufactured plastic types requires verification. Changes in hydroxyl and carbon-oxygen bonds are most readily diagnosed by FTIR, followed by carbonyl bonds.

Application of the chronology of changes in experimentally weathered particles to microplastic collected in the open ocean suggests that the PE particles we sampled in the California Current and transition region may have generally weathered for under 18 months, in contrast to the particles from the North Pacific Subtropical Gyre that generally had inferred exposure times longer than 18 months. The indices tested here proved more applicable for comparing oceanic and experimental values of PE than PP, and were the most useful for HDPE. These findings are consistent with oceanic circula-

tion models suggesting a long residence time of suspended micro-plastics in the open ocean.

Acknowledgements

We thank Pacific Plastics Injection Molding, Damar Plastics, P. Dinger, and C. Rochman for their donation of preproduction plastic pellets. G. Arrhenius, M.J. Sailor, J. Lee, N. Chan, and A. Potocny made the FTIR work possible. We thank M.J. Sailor, L. Aluwihare, and M. Landry for comments on the manuscript. We thank NOAA NDBC for temperature data. We are grateful to K.E. Armaiz for assistance in the laboratory, P. Zerofski for help with experimental setup, J. Ellen for help with Python, E. Jacobson and J. Carriere-Garwood for help with R, and the numerous volunteers who helped JAB clean tanks. Funding for the SEAPLEX cruise was provided by University of California Ship Funds, Project Kaisei/Ocean Voyages Institute, AWIS-San Diego, and NSF IGERT Grant No. 0333444. MCG was supported by NSF GK-12 Grant No. 0841407 and donations from Jim & Kris McMillan, Jeffrey & Marcy Krinsk, Lyn & Norman Lear, Ellis Wyer, and an anonymous donor, and JAB was supported by donations from the Furlotti Family. This work was also funded by a contribution from the California Current Ecosystem LTER site, supported by NSF Award No. 1026607.

Appendix A. Supplementary data

Supplementary data to this article can be found online at http://dx.doi.org/10.1016/j.marpolbul.2016.06.048.

References

Abbate, S., Gussoni, M., Zerbi, G., 1979. Infrared and Raman intensities of polyethylene and perdeuteropolyethylene: factor group splittings. J. Chem. Phys. 70, 3577–3585.

Albertsson, A.-C., Andersson, S.O., Karlsson, S., 1987. The mechanism of biodegradation of polyethylene. Polym. Degrad. Stab. 18, 73–87.

American Chemistry Council, 2010. Resin identification codes. In: http://www.americanchemistry.com/s_plastics/doc.asp?CID=1102&DID=4644.

Andrady, A.L., 1990. Weathering of polyethylene (LDPE) and enhanced photodegradable polyethylene in the marine environment. J. Appl. Polym. Sci. 39, 363–370.

Andrady, A.L., 2003. Common plastics materials. In: Andrady, A.L. (Ed.), Plastics and the Environment. John Wiley & Sons, Hoboken, NJ, pp. 77–121.

Andrady, A.L., 2011. Microplastics in the marine environment. Mar. Pollut. Bull. 62, 1596–1605.

Andrady, A., Pegram, J., Tropsha, Y., 1993. Changes in carbonyl index and average molecular weight on embrittlement of enhanced-photodegradable polyethylenes. Journal of Environmental Polymer Degradation 1, 171–179.

Avitabile, G., Napolitano, R., Pirozzi, B., Rouse, K.D., Thomas, M.W., Willis, B.T.M., 1975. Low temperature crystal structure of polyethylene: results from a neutron diffraction study and from potential energy calculations. Journal of Polymer Science: Polymer Letters Edition 13, 351–355.

Brown, D., Cheng, L., 1981. New net for sampling the ocean surface. Mar. Ecol. Prog. Ser. 5, 224–227.

Browne, M.A., Dissanayake, A., Galloway, T.S., Lowe, D.M., Thompson, R.C., 2008. Ingested microscopic plastic translocates to the circulatory system of the mussel, Mytilus edulis (L.). Environ. Sci. Technol. 42, 5026–5031.

CalRecycle, 2016. In: C. D. o. R. R. a. R. (CalRecycle) (Ed.), Biannual Report of Beverage Container Sales, Returns, Redemption, and Recycling Rates. California Environmental Protection Agency (http://www.calrecycle.ca.gov/bevcontainer/Notices/2016/Biannual.pdf).

Carlsson D.J., Dobbin C.J.R., Jensen J.P.T., and D.M. Wiles, Polypropylene degradation by g-irradiation in air, ACS Symposium Series, **280**, 1985.Carpenter, E.J., Smith, K., 1972. Plastics on the Sargasso Sea surface. Science 175, 1240–1241.

Cole, M., Lindeque, P., Fileman, E., Halsband, C., Goodhead, R., Moger, J., Galloway, T.S., 2013. Microplastic ingestion by zooplankton. Environ. Sci. Technol. 47, 6646–6655.

Conservancy, O., 2010. Trash Travels. International Coastal Cleanup 25th Anniversary Report. .

Corrales, T., Catalina, F., Peinado, C., Allen, N., Fontan, E., 2002. Photooxidative and thermal degradation of polyethylenes: interrelationship by chemiluminescence, thermal gravimetric analysis and FTIR data. J. Photochem. Photobiol. A Chem. 147, 213–224.

Davison, P., Asch, R.G., 2011. Plastic ingestion by mesopelagic fishes in the North Pacific Subtropical Gyre. Mar. Ecol. Prog. Ser. 432, 173–180.

Dotson, A., Magaard, L., Niemeyer, G., Wyrtki, K., 1977. A Simulation of the Movements of Fields of Drifting Buoys in the North Pacific Ocean. Hawaii Institute of Geophysics, University of Hawaii.

El-Ghaffar, M.A., Youssef, E., Darwish, W., Helaly, F., 1998. A novel series of corrosion inhibitive polymers for steel protection. Journal of Elastomers and Plastics 30, 68–94.

EPA. 2014. Municipal Solid Waste Generation, Recycling, and Disposal in the United States: Tables and Figures for 2012. In U. S. E. P. Agency, editor (Washington D.C. USA).

Eriksen, M., Lebreton, L.C., Carson, H.S., Thiel, M., Moore, C.J., Borerro, J.C., Galgani, F., Ryan, P.G., Reisser, J., 2014. Plastic pollution in the world's oceans: More than 5 trillion plastic pieces weighing over 250,000 tons afloat at sea. PLoS One 9, e111913.

Eriksson, C., Burton, H., 2003. Origins and biological accumulation of small plastic particles in fur seals from Macquarie Island. AMBIO: A Journal of the Human Environment 32, 380–384.

Forrest, M., Davies, Y., Davies, J., 2007. The Rapra Collection of Infrared Spectra of Rubbers, Plastics and Thermoplastic Elastomers. Smithers Rapra Publishing.

Freund Container & Supply, 2010. Plastic Properties. Guide to Plastics. .

Frias, J.P.G.L., Sobral, P., Ferreira, A.M., 2010. Organic pollutants in microplastics from two beaches of the Portuguese coast. Mar. Pollut. Bull. 60, 1988–1992.

Goldstein, M.C., Goodwin, D.S., 2013. Gooseneck barnacles (Lepas spp.) ingest microplastic debris in the North Pacific Subtropical Gyre. Peer J. 1, e184.

Goldstein, M.C., Titmus, A.J., Ford, M., 2013. Scales of spatial heterogeneity of plastic marine debris in the northeast Pacific ocean. PLoS One 8, e80020.

Gulmine, J., Janissek, P., Heise, H., Akcelrud, L., 2002. Polyethylene characterization by FTIR. Polym. Test. 21, 557–563.

Hidalgo-Ruz, V., Gutow, L., Thompson, R.C., Thiel, M., 2012. Microplastics in the marine environment: a review of the methods used for identification and quantification. Environ. Sci. Technol. 46, 3060–3075.

International, A., 2011. ASTM Standard C702/C702M-11. Practice for Reducing Samples of Aggregate to Testing Size. (West Conshohocken, PA).

Ioakeimidis, C., Fotopoulou, K., Karapanagioti, H., Geraga, M., Zeri, C., Papathanassiou, E., Galgani, F., Papatheodorou, G., 2016. The degradation potential of PET bottles in the marine environment: an ATR-FTIR based approach. Sci. Report. 6.

Jabarin, S.A., Lofgren, E.A., 1994. Photooxidative effects on properties and structure of high-density polyethylene. J. Appl. Polym. Sci. 53, 411–423.

Jambeck, J.R., Geyer, R., Wilcox, C., Siegler, T.R., Perryman, M., Andrady, A., Narayan, R., Law, K.L., 2015. Plastic waste inputs from land into the ocean. Science 347, 768–771.

Kubota, M., 1994. A mechanism for the accumulation of floating marine debris north of Hawaii. J. Phys. Oceanogr. 24, 1059–1064.

Kubota, M., Takayama, K., Namimoto, D., 2005. Pleading for the use of biodegradable polymers in favor of marine environments and to avoid an asbestos-like problem for the future. Appl. Microbiol. Biotechnol. 67, 469–476.

La Mantia, F.P., Morreale, M., 2008. Accelerated weathering of polypropylene/wood flour composites. Polym. Degrad. Stab. 93, 1252–1258.

Lacoste, J., Carlsson, D., 1992. Gamma-, photo-, and thermally-initiated oxidation of linear low density polyethylene: a quantitative comparison of oxidation products. J. Polym. Sci. A Polym. Chem. 30, 493–500.

Livanova, N., Zaikov, G., 1992. A scale effect in the durability of oriented narrow polypropylene films during oxidation under load. Fracture model of stressed polypropylene films. Polym. Degrad. Stab. 36, 253–259.

Lobo, H., Bonilla, J.V., 2003. Handbook of Plastics Analysis. Crc Press.

Lynn, R.J., Simpson, J.J., 1987. The California Current System: the seasonal variability of its physical characteristics. Journal of Geophysical Research: Oceans (1978–2012) 92, 12947–12966.

Ma, X., Lu, J.Q., Brock, R.S., Jacobs, K.M., Yang, P., Hu, X.-H., 2003. Determination of complex refractive index of polystyrene microspheres from 370 to 1610 nm. Phys. Med. Biol. 48, 4165.

Markelz, A., Roitberg, A., Heilweil, E., 2000. Pulsed terahertz spectroscopy of DNA, bovine serum albumin and collagen between 0.1 and 2.0 THz. Chem. Phys. Lett. 320, 42–48.

Maximenko, N., Hafner, J., Niiler, P., 2012. Pathways of marine debris derived from trajectories of Lagrangian drifters. Mar. Pollut. Bull. 65, 51–62.

Murray, F., Cowie, P.R., 2011. Plastic contamination in the decapod crustacean Nephrops norvegicus (Linnaeus, 1758). Mar. Pollut. Bull. 62, 1207–1217.

Niiler, P.P., Reynolds, R.W., 1984. The three-dimensional circulation near the eastern North Pacific Subtropical Front. J. Phys. Oceanogr. 14, 217–230.

Ogata, Y., Takada, H., Mizukawa, K., Hirai, H., Iwasa, S., Endo, S., Mato, Y., Saha, M., Okuda, K., Nakashima, A., Murakami, M., Zurcher, N., Booyatumanondo, R., Zakaria, M.P., Dung, L.Q., Gordon, M., Miguez, C., Suzuki, S., Moore, C., Karapanagioti, H.K., Weerts, S., McClurg, T., Burres, E., Smith, W., Velkenburg, M.V., Lang, J.S., Lang, R.C., Laursen, D., Danner, B., Stewardson, N., Thompson, R.C.,

2009. International Pellet Watch: global monitoring of persistent organic pollutants (POPs) in coastal waters. 1. Initial phase data on PCBs, DDTs, and HCHs. Mar. Pollut. Bull. 58, 1437–1446.
Pavia, D., Lampman, G., Kriz, G., Vyvyan, J., 2008. Introduction to Spectroscopy. Cengage Learning.
Pegram, J.E., Andrady, A.L., 1989. Outdoor weathering of selected polymeric materials under marine exposure conditions. Polym. Degrad. Stab. 26, 333–345.
Piesiewicz, R., Jansen, C., Wietzke, S., Mittleman, D., Koch, M., Kürner, T., 2007. Properties of building and plastic materials in the THz range. International Journal of Infrared and Millimeter Waves 28, 363–371.
Rabello, M., White, J., 1997. The role of physical structure and morphology in the photodegradation behaviour of polypropylene. Polym. Degrad. Stab. 56, 55–73.
Rajakumar, K., Sarasvathy, V., Chelvan, A.T., Chitra, R., Vijayakumar, C., 2009. Natural weathering studies of polypropylene. J. Polym. Environ. 17, 191–202.
Reddy, M.S., Shaik, B., Adimurthy, S., Ramachandraiah, G., 2006. Description of the small plastics fragments in marine sediments along the Alang-Sosiya ship-breaking yard, India. Estuar. Coast. Shelf Sci. 68, 656–660.
Rios, L.M., Moore, C., Jones, P.R., 2007. Persistent organic pollutants carried by synthetic polymers in the ocean environment. Mar. Pollut. Bull. 54, 1230–1237.
Rochman, C.M., Hoh, E., Kurobe, T., Teh, S.J., 2013. Ingested plastic transfers hazardous chemicals to fish and induces hepatic stress. Sci. Report. 3.
Roden, G.I., 1980. On the subtropical frontal zone north of Hawaii during winter. J. Phys. Oceanogr. 10, 342–362.
Rodriguez-Gonzalez, F.J., Ramsay, B.A., Favis, B.D., 2003. High performance LDPE/thermoplastic starch blends: a sustainable alternative to pure polyethylene. Polymer 44, 1517–1526.
Roy, P., Surekha, P., Rajagopal, C., 2011. Surface oxidation of low-density polyethylene films to improve their susceptibility toward environmental degradation. J. Appl. Polym. Sci. 122, 2765–2773.
Samuels, R.J., 1981. Application of refractive index measurements to polymer analysis. J. Appl. Polym. Sci. 26, 1383–1412.
Siegel, S., Castellan, N.J.J., 1988. Non Parametric Statistics for the Behavioural Sciences. MacGraw Hill International, New York.
Socrates, G., 2004. Infrared and Raman Characteristic Group Frequencies: Tables and Charts, third ed. John Wiley & Sons, Ltd., Chichester, England.
Stark, N.M., Matuana, L.M., 2004. Surface chemistry changes of weathered HDPE/wood-flour composites studied by XPS and FTIR spectroscopy. Polym. Degrad. Stab. 86, 1–9.
Tadokoro, H., Kobayashi, M., Ukita, M., Yasufuku, K., Murahashi, S., Torii, T., 1965. Normal vibrations of the polymer molecules of helical conformation. V. Isotactic polypropylene and its deuteroderivatives. J. Chem. Phys. 42, 1432–1449.
Thompson, R.C., Olsen, Y., Mitchell, R.P., Davis, A., Rowland, S.J., John, A.W., McGonigle, D., Russell, A.E., 2004. Lost at sea: where is all the plastic?. Science 304, 838.
Tidjani, A., 2000. Comparison of formation of oxidation products during photo-oxidation of linear low density polyethylene under different natural and accelerated weathering conditions. Polym. Degrad. Stab. 68, 465–469.
Wong, C., Green, D.R., Cretney, W.J., 1974. Quantitative tar and plastic waste distributions in the Pacific Ocean. Nature 247, 30–32.
Workman Jr., J., Springsteen, A., 1998. Applied Spectroscopy: A Compact Reference for Practitioners. Academic Press.
Wright, S.L., Thompson, R.C., Galloway, T.S., 2013. The physical impacts of microplastics on marine organisms: a review. Environ. Pollut. 178, 483–492.
Zerbi, G., Gallino, G., Del Fanti, N., Baini, L., 1989. Structural depth profiling in polyethylene films by multiple internal reflection infra-red spectroscopy. Polymer 30, 2324–2327.